[1,2]Jing Zhang

[1,2]Yonghui Yin

[1,2]Pengfei Zhao

Research on Multiple Big Data Fusion Techniques in Geographic Information System (GIS)

JES Journal of Electrical Systems

Abstract: - Geographic Information System (GIS) has many different types of data sources, and realizing the fusion of heterogeneous data from multiple sources can enhance the application areas of GIS. This paper establishes a geographic information system based on C/S and B/S modes, and designs a database storage module and a fusion mechanism for multi-source data. Multiview image preprocessing technology is used to optimize the UAV tilt measurement image, the light component of the geographic information image is accurately and quickly extracted by fast guided filtering algorithm, and linear stretching is introduced to image enhancement of remote sensing data. Then, combining the SIFT algorithm to align the features of the geographic information image and fusing the remote sensing image and the UAV image by using the IHS transform, the fusion processing flow of multi-source heterogeneous data is designed. For the effectiveness of the fusion of multi-source big data, it is verified from the alignment of geographic information images and the fusion of multi-source heterogeneous data, respectively. It is found that the time consumption of SIFT algorithm in geographic information image alignment is only 1.241s, and the accuracy of image feature point matching is 88.44%.The CC and EN values of IHS data fusion are 0.924 and 7.652 respectively, and the modeling error of geographic information 3D model is between [0.01m,0.07m]. Through the effective fusion of multi-source big data, the three-dimensional display of geographic information by GIS system can be realized to provide support for geographic information exploration.

Keywords: geographic information system; fast oriented filtering; linear stretching; SIFT algorithm; IHS transform; multi-source data fusion

1. Introduction

With the rapid development of spatial database technology, human beings have accumulated a large amount of spatial data, and the wide application of geographic information systems (GIS), remote sensing, and medical imaging has led to the dramatic generation and increase of spatial data [1-2]. For example, the National Aeronautics and Space Administration (NASA) Earth Observation System (EOS) generates 1 TB of spatial data every day [3]. The large-scale geospatial databases and thematic databases built in China covering the whole country and province have a total data volume of more than 1250 GB [4]. Regarding fire data, terrain distribution data, etc., a large amount of spatial data with a wide variety of data types and features have been collected. According to statistics, the amount of data owned globally doubles every 20 months, so we not only have an extremely large amount of spatial data, but its spatial data types are becoming more and more complex and diverse in structure [5-6]. The increasing abundance of data with spatial characteristics has exceeded the analytical ability of the human brain to a certain extent, thus forming a situation in which spatial data, although abundant, are poor in knowledge and of little use [7].

[1] Yantai Center of Coastal Zone Geological Survey, China Geological Survey, Yantai 264000, Shandong, China

[2] Ministry of Natural Resources Observation and Research Station of Land-Sea Interaction Field in the Yellow River Estuary, Yantai 264000, Shandong,China.*Email:bingguojingjing@163.com

Spatial multivariate big data fusion refers to the extraction and fusion of non-explicit existent knowledge, spatial relationships or other meaningful patterns in spatial databases [8]. Spatial data fusion requires integrated data fusion, spatial databases, spatial informatics, computer science and other techniques. It can be used for the understanding of spatial data, discovery of spatial relationships and relationships between spatial and non-spatial data, construction of spatial knowledge bases, adequacy of spatial databases and optimization of spatial queries [9]. Spatial data fusion in general can be categorized into spatial association rule techniques, spatial congruence, spatial outlier techniques, spatial classification, and spatio-temporal sequences [10]. It has a wide range of applications in many fields that use spatial data such as GIS, geo-marketing, remote sensing, CAD, image database detection, navigation, traffic control, environmental studies, etc [11-13]. Due to the huge amount of spatial data, the complexity of spatial data types and spatial access methods, the study of efficient spatial data fusion technology has become an inevitable development with full consideration of spatial relevance.

The GIS system constructed in this paper is an application system mainly in C/S mode and supplemented by B/S mode, for which a data storage method based on the mixed management of file system and database is also designed, and the fusion mechanism of multi-source data is explored. Multi-source data fusion is required in the data layer of the GIS system. In this paper, multi-view image preprocessing is utilized to correct the aberration difference and homogenize the light and color of the UAV tilt measurement image, and the light component of the geographic information image is extracted by the fast bootstrap filtering algorithm. Combined with the linear stretching method for image enhancement processing of geographic information images acquired by remote sensing technology, based on the SIFT algorithm, the geographic information is divided into three-dimensional grids to realize the alignment calculation of geographic information three-dimensional model. After acquiring multi-source geographic information images, the remote sensing images and UAV images were fused using HIS transform, and the data fusion processing flow was designed. Finally, the effectiveness of multi-source big data fusion technology is verified from the dimensions of geographic information image feature alignment, multi-source data fusion experiment, and geographic information 3D reconstruction.

2. GIS framework design

Geographic Information System (GIS) is mainly composed of three parts, which are computer system, geographic data and user system, which are indispensable, and its utilization is mainly the collection, storage, management and processing of data. The traditional data collection is the survey and mapping personnel through the field survey measurements and finally come to a conclusion, which spends a lot of time, and the data is not accurate enough, while GIS does not need to worry about such problems. The use of computer software can not only process many data accurately, but also provide multiple reference programs for builders, adding new vitality to geographic environment analysis and regional construction.

2.1 General framework of GIS

The overall framework design of GIS is shown in Figure 1. In this paper, the system adopts "C/S+B/S" mixed structure application system, that is, C/S mode as the main, B/S mode as a complementary geographic information system. This ensures that the system is efficient, stable operation, but also to meet the user requirements of the system. The C/S mode is mainly used for geographic information query, path planning, map mapping and three-dimensional display, etc., and the B/C mode is used for other auxiliary functions such as publicity and promotion. The system architecture adopts the four-layer structure of foundation layer, data layer, application layer and user layer. The user layer is the system service object, such as tourists, the public and administrators. The application layer contains various functions provided by the system, i.e. login and registration, basic map operation, information query, route planning, map decoration and cartography, and auxiliary functions. The data layer contains thematic spatial data and attribute data in the basic geographic database, geographic service database,

geographic resource database, image database and multimedia database, and the foundation layer contains related supporting software and hardware facilities and development environment.

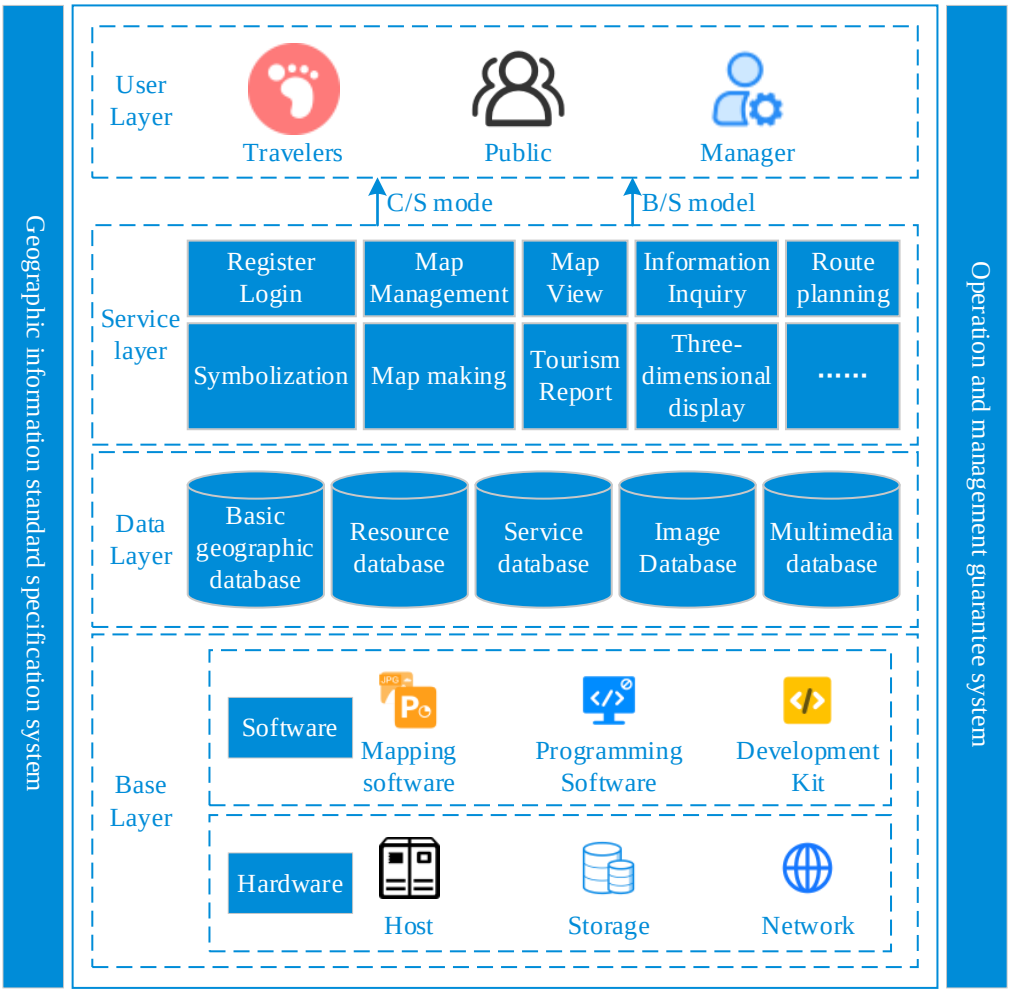

Figure 1 The overall framework of GIS

2.2 Database storage module

The GIS database developed in this paper contains spatial and temporal data with different data specifications and different data models, such as soil, river, highway, etc., and we need to store and manage these data in a unified way. For the management of spatial data, GIS takes the following approaches:

(1) file-based approach, which uses file system to store and manage spatial data, simple operation, intuitive and convenient. However, it can only store a limited amount of spatial data, which cannot meet the demand of massive data nowadays.

(2) The hybrid management method based on file system and database, which uses the traditional relational database system to store the attribute data of geospatial objects and files to store spatial data.

(3) Management based on spatial database, which can directly construct database system used to store and manage spatial data and attribute data to manage data. The database directly supports the storage and management of spatial objects and provides an efficient query and retrieval mechanism for spatial data.

In this regard, this paper adopts the mixed management of file system and database, with spatial data stored in the file system and non-spatial data stored in the relational database. For this reason, it is necessary to associate the spatial and non-spatial data information stored separately, and the association of spatial data and attribute data is shown in Figure 2, which is mainly through the geocode to complete the data association. Geocode is the keyword

to link graphical data and attribute data, which can indicate the geographic location of the object and the containment relationship, and it is unique in the system.

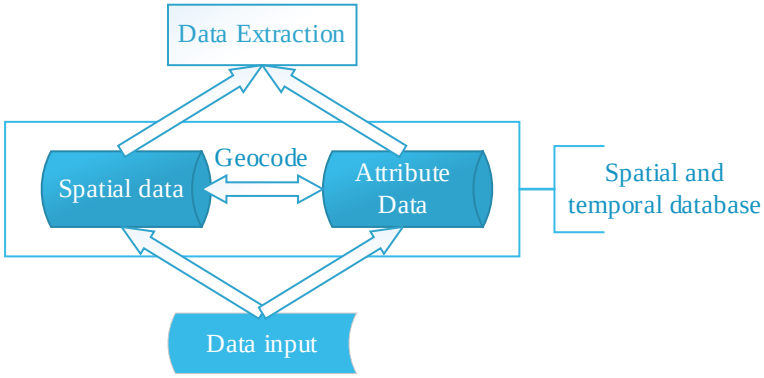

Figure 2 The correlation between spatial data and attribute data

2.3 Multi-source data fusion mechanisms

Following the system design idea, starting from the business logic unit that constitutes the system, the data fusion method is divided into four levels of information application, information pooling, information storage and information collection according to the principle of structural layering for construction. The multivariate data fusion mechanism is shown in Figure 3. The information provision in business applications is realized by the data convergence platform, and the business applications cover different geographic information business application systems and comprehensive information service systems. The information aggregation layer provides real-time geographic information and comprehensive management information aggregation functions for the whole GIS. The information storage layer realizes data processing, storage and sharing. The information collection layer realizes the collection and reporting of real-time geographic information and the uploading of comprehensive management information.

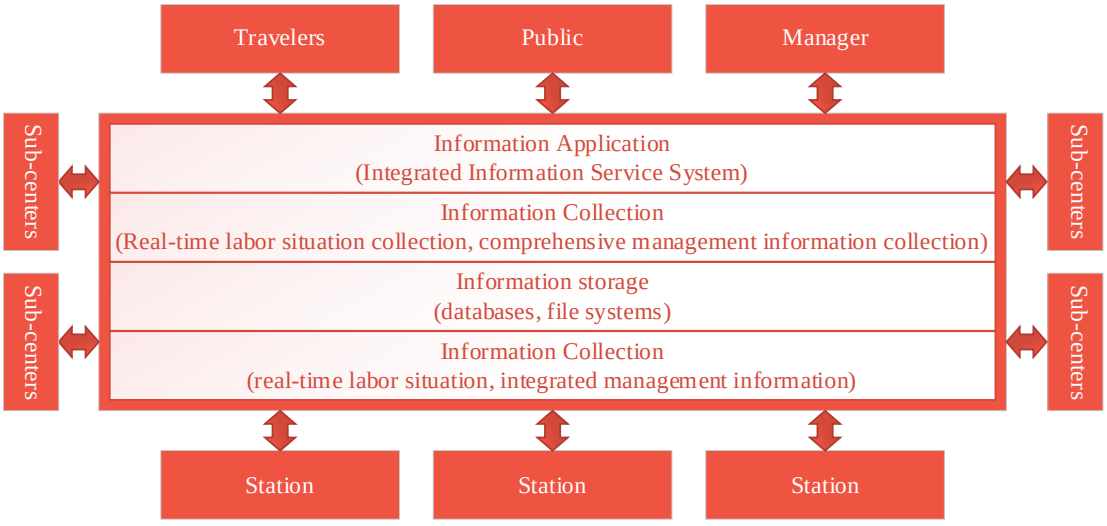

Figure 3 Multiple data fusion mechanism

Among the main functions include:

(1) Data collection function

Real-time collection of geo-environmental information, realizing the reception (decryption), (encryption) distribution, processing and storage of geo-environmental information.

(2) Data collection management

Improve the process monitoring and statistical analysis of data collection. The main task of the data collection platform is to complete the information exchange between the nodes. In order to ensure the safety of information transmission, the different stages of information transmission can be monitored in real time. Data collection platform communication software is built on top of the TCP protocol using middleware technology, and shall not be developed on top of the UDP protocol.

3. Multi-dimensional big data fusion model

The geographic information system integrates spatial data and attribute data and other multifaceted data under the joint effect of big data technology and remote sensing mapping technology. It plays the advantages of data measurement automation and data analysis intelligence in geographic information survey and urban mapping, improves the working efficiency as well as the comprehensiveness and accuracy of the acquired data, and makes the geographic information management more scientific, refined, digitalized and intelligent. Therefore, the effective integration of multi-source big data in GIS can further optimize the efficient application of GIS and realize the precise grasp of geographic environment information.

3.1 Geographic information three-dimensional modeling technology

3.1.1 Multiview image preprocessing

In geographic information systems, geographic information data are collected in order to better realize the three-dimensional display of geographic information. Inclined photogrammetry is usually equipped with a non-metric camera, which cannot accurately determine the internal orientation elements and the lens group is not closely calibrated, resulting in optical defects such as aberrations and other optical defects in the image taken by the non-metric camera. Especially in high mountainous terrain, it is easy to have problems such as image point displacement and large image edge aberrations, so it is necessary to pre-process the image from multiple angles, which usually includes aberration correction and image homogenization and color homogenization.

(1) Aberration correction

The aberration on the photographic objective lens affects the parallelism of the outgoing and incoming rays at the same time, resulting in the image point deviating from the theoretical position and failing to satisfy the three-point covariance relationship between the image point, the object point, and the center of photography. Therefore, it is not possible to calculate the coordinates of the image point corresponding to the object point using the equation of the covariance condition, which is caused by the existence of aberrations in the objective lens. Optical aberrations are usually categorized into three types, i.e., radial aberrations, tangential aberrations, and CCD facet distortion. Specific correction methods are as follows:

Radial aberrations are mainly caused by imperfections in the lens group in the camera, and the repair formula for radial aberrations is usually expressed as:

$$\begin{cases} \Delta x_r = x_0\left(k_1 r^2 + k_2 r^4 + k_3 r^6\right) \\ \Delta y_r = x_0\left(k_1 r^2 + k_2 r^4 + k_3 r^6\right) \end{cases} \tag{1}$$

Where $r = \sqrt{x_0^{\,2} + y_0^{\,2}}$ is the radial direction, $\left(x_0 + y_0\right)$ represents the image coordinates of the main point of the image as the origin, K_1, K_2, K_3 represents the aberration parameter of the camera lens, and $\Delta x, \Delta y$ represents the aberration difference of the image point x, y.

Tangential aberration is caused by the direction of displacement of the image point is perpendicular to the radial direction, tangential aberration correction formula is usually expressed as:

$$\begin{cases} \Delta x_d = P_1\left(r^2 + 2x_0^2\right) + 2P_2 x_0 y_0 \\ \Delta y_d = P_1\left(r^2 + 2y_0^2\right) + 2P_2 x_0 y_0 \end{cases} \tag{2}$$

where P_1, P_2 represents the tangential distortion parameter of the camera lens.

The correction formula for the CCD face distortion is given by:

$$\begin{cases} x_f = \alpha x_0 + \beta y_0 \\ y_f = 0 \end{cases} \tag{3}$$

where α, β denotes the correction parameter for the camera lens aberration difference.

The sum of the above three aberrations is the correction of camera aberration, then:

$$\begin{cases} \Delta x = x_r + x_d + x_f \\ \Delta y = y_r + y_d + y_f \end{cases} \tag{4}$$

If you need to correct the image aberration difference, you can use the camera calibration software to check the camera calibration, you can get the above seven aberration parameters and bring them into the aberration correction formula, you can get x, y, z three directions on the corrected value.

(2) Even light and color processing

When the drone collects images, it will be affected by many factors, such as weather, sunlight, shooting time and the camera itself, resulting in uneven brightness and color among the collected image data, which causes color difference between the indirect edges of the image in the process of splicing, or the same image has a large difference in color and a large difference in the distribution of light, which will have an impact on the construction and application of the subsequent three-dimensional model. This will have an impact on the construction and application of the subsequent three-dimensional model. Therefore, it is necessary to equalize the light and color of UAV images.

The basic idea of the Wallis filter-based homogenization algorithm is to process the image to be processed by using the variance and the mean gray value of the reference image, so that the image to be processed will have similar mean gray value and variance, thus achieving the purpose of image homogenization. Its linear transformation equation is as follows:

$$f(x, y) = g(x, y) r_1 + r_0 \tag{5}$$

Where $g(x, y)$ denotes the gray value of the initial image at (x, y), $f(x, y)$ denotes the gray value of the linearly transformed image at (x, y), r_1 denotes the multiplicative coefficient in the linear transformation, and r_0 is the additive coefficient in the linear transformation. Then:

$$\begin{cases} r_0 = b m_f + (1-b) m_g \\ r_1 = \dfrac{c s_f}{c s_g + (1-c) s_f} \end{cases} \tag{6}$$

Where, m_g denotes the local gray mean of the initial image, s_g denotes the corresponding standard deviation,

m_f denotes the target value of the local gray mean of the resultant image, and s_f denotes the target value of the affected local gray deviation of the corresponding result. $c \in [0,1]$ denotes the dilation constant of the image variance, and $b \in [0,1]$ denotes the luminance coefficient of the image. When the values of b and c are both 1, the linear transformation formula is as follows:

$$f(x,y) = \left[g(x,y) - m_g \right] \frac{s_f}{s_g} + m_f \tag{7}$$

If Eq. $m_s = m_f, s_g = s_f$, the image gray value remains unchanged when the linear transformation is changed.

3.1.2 Extracting geographic information light components

According to the illumination-reflection imaging model, the brightness of an image is jointly affected by the illumination component and the object reflection component. Therefore, in order to solve the problem of uneven illumination existing in the image, it is very important to accurately extract the illumination information in the image. The guided filtering algorithm can recalculate each pixel value within the filtering window by guiding the linear relationship between the image and the input image to obtain the low frequency information in the image. The light component extracted using this algorithm is closest to the original luminance image, so in this paper we use fast guided filtering algorithm to accurately and quickly extract the light component of geographic information.

The basic idea of bootstrap filtering is that the input image p, the bootstrap image I, and the filtered output image q, on the current pixel point k, all of which exist in a filter window w_k centered at point k and radiused at point r, exhibit the following linear transformation relationship. Namely:

$$q_i = a_k I_i + b_k, \forall i \in w_k \tag{8}$$

Where a_k, b_k are linear transformation factors, which are constants within the window. The central idea of bootstrap filtering is to calculate the optimal value of a_k, b_k within the window to minimize the difference between the input image p and the filtered output image q. The solution of the optimal value of a_k, b_k can be expressed as:

$$a_k = \frac{\frac{1}{|w|}\sum_{i \in w_k} I_i p_i - \mu_k \overline{p_k}}{\sigma_k^2 + \varepsilon} \tag{9}$$

$$b_k = \overline{p_k} - a_k \mu_k \tag{10}$$

Where $|w|$ is the number of pixels in the window, σ and μ are the mean and variance of the bootstrap image I, and ε is the value of the regularization parameter that prevents the value from being too large. Substituting Eq. (9) and Eq. (10) into Eq. (8), it can be obtained:

$$q_i = \frac{1}{|\omega|}\sum_{i\in w_k}\left(a_k I_i + b_k\right) = \overline{a}_i I_i + \overline{b_i} \tag{11}$$

Guided filtering can maximize the retention of the input image features, effectively obtain the details of the bootstrap image changes, and has good edge preservation characteristics. And fast guided filtering is based on this with s times downsampling of the input image and the guided image to solve a_k, b_k, further reducing the time cost, can be fast, accurate and efficient extraction of geographic information of the intensity of the light component.

3.1.3 Remote sensing image enhancement processing

In addition to applying drones to obtain real images of geographic information, this paper also uses remote sensing technology to obtain remote sensing image data of relevant areas. Since the satellite remote sensing images are interfered by many factors in the imaging process, such as changes in the height and pose angle of the remote sensors, atmospheric refraction, curvature of the Earth, terrain undulation, rotation of the Earth, rotation of the Earth in the process of dynamic scanning of the remote sensors, and changes in the structural properties of the remote sensors themselves, etc., this paper adopts the linear stretching method to enhance the remote sensing images. Therefore, in this paper, linear stretching is used to enhance the remote sensing image.

Linear stretching is based on the original image histogram to determine the gray value interval before the stretching transformation, and then this gray value interval is stretched or compressed according to a linear equation and becomes the gray value interval after the transformation, so as to improve the contrast and clarity of the image, highlight the details of the image, and make it easy to read all kinds of features. The transformation formula used for linear transformation is:

$$g(x,y) = T[f(x,y)] = A + B \bullet f(x,y) \tag{12}$$

Where T is the transformation function, A and B are the transformation parameters, which are determined by the dynamic range of the gray value of the original image and the transformed image.

After the linear stretching process, the gray value range of the remote sensing image is stretched from 0 to 164 to 0 to 255 before the enhancement process, which enhances the visual interpretation of geographic information.

3.2 Distributed Geographic Information Alignment Algorithm

3.2.1 Scale-invariant feature transformation

When analyzing the acquired multi-source data in GIS, it is necessary to effectively align the related data of the same category, so as to facilitate better comparative analysis. Therefore, in this paper, the scale invariant feature transformation (SIFT) algorithm is used to collect the feature points of multi-source data images and the angle information carried by the feature points to realize the multi-source data alignment of geographic information.The SIFT algorithm is invariant to the image scale, illumination, and rotation, and has strong stability, which is capable of extracting sufficient and reliable feature points in a complex environment. The steps of the algorithm are as follows:

(1) Scale space extreme value detection

The algorithm utilizes the Gaussian differential function to detect the extreme points in the image that are invariant to scale and rotation. Let $I(x,y)$ be the original image function, the scale space $L(x,y,\sigma)$ of the image is obtained by convolving the Gaussian differential function with the original image, and its expression is:

$$L(x,y,\sigma) = G(x,y,\sigma) * I(x,y) \tag{13}$$

Where $G(x,y,\sigma)$ is the Gaussian function fuzzy function with the expression:

$$G(x,y,\sigma)=\frac{1}{2\pi\sigma^2}e^{\frac{-\left(x^2+y^2\right)}{2\sigma^2}} \tag{14}$$

where σ is the spatial scale and this parameter indicates the degree of Gaussian blurring of the image.
Then the spatial extremes are detected using Difference of Gaussian (DOG) with the following expression:

$$\begin{aligned} D(x,y,\sigma)&=(G(x,y,k\sigma)-G(x,y,\sigma))\otimes I(x,y)\\ &=L(x,y,k\sigma)-L(x,y,\sigma)\end{aligned} \tag{15}$$

where $D(x,y,\sigma)$ is the Gaussian difference function and k is the scale factor of two neighboring scale spaces $(k=\sqrt{2})$.

(2) Precise localization of key points

The spatial extreme points obtained in the previous step are unreliable feature points, and some of the extreme points satisfy the conditions of Gaussian difference extrema but are not real feature points. Expand the Gaussian difference function at the feature points with Taylor's formula to improve the stability of the feature points. The expression is as follows:

$$D(X)=D+\frac{\partial D^T}{\partial X}X+\frac{1}{2}X^T\frac{\partial^2 D}{\partial X^2}X \tag{16}$$

Eq. $X=(x,y,\sigma)^T$. The extraction of keypoints by the above method produces a strong edge response, and unstable extreme points can be eliminated by setting a threshold.

(3) Feature point direction assignment

The extreme points obtained in the above two steps need to calculate the gradient values and gradient directions of other pixel points in their neighborhood. The calculation formula is as follows:

$$m(x,y)=\sqrt{(L(x+1,y)-L(x-1,y))^2+(L(x,y+1)-L(x,y-1))^2} \tag{17}$$

$$\theta(x,y)=\tan^{-1}\frac{L(x,y+1)-L(x,y-1)}{L(x+1,y)-L(x-1,y)} \tag{18}$$

where m is the gradient value and θ is the gradient direction.

After calculating the gradient values and directions of other points in the neighborhood, firstly, the gradient directions of all pixel points are counted and a histogram is drawn, and then the wave peaks of the histogram are found in the graph, and its direction is taken as the main direction of the feature point.

(4) Generate feature point descriptor

The above steps get the localization, scale and direction of the feature points. It is necessary to create a descriptor for all feature points, which not only needs to include the relevant information of the feature points, but also ensures the uniqueness of the descriptor, in order to improve the accuracy of feature point matching.

Suppose $T=(t_1,t_2,\ldots,t_{128})$ is a 128-dimensional feature descriptor of a feature point, which needs to be normalized in order to eliminate the effect of light variations. The normalized feature vector can be expressed as:

$$\bar{t}_i = \frac{t_i}{\sqrt{\sum_{j=1}^{128} t_j}} \tag{19}$$

The feature descriptor obtained after normalization is $T = \left(\bar{t}_1, \bar{t}_2, \ldots, \bar{t}_{128}\right)$.

3.2.2 Geographic Information Alignment Computing Cluster

In order to display geographic information in three dimensions in GIS, it is necessary to realize the effective alignment of three-dimensional information, and the distributed geographic alignment computation cluster can combine the geographic information alignment computation units, so as to obtain a more accurate three-dimensional model of geographic information. Each geographic alignment computing unit takes the top view of the 3D model and a remote sensing image window slice as inputs, and finally realizes the geographic alignment of the 3D model by calculating the pixel coordinate conversion matrix between the top view of the 3D model and a remote sensing image slice. In the distributed geographic alignment computing cluster, each geographic alignment computing unit has three computing stages. The details are as follows:

(1) First computational stage

Each geographic alignment computation unit utilizes the SIFT-based algorithm to compute the same feature points between the 3D model top view and the remote sensing image slices. Denote by ϕ the set of all identical feature point pairs between the top view of the 3D model and the remote sensing image window slice computed by the feature point-based image matching algorithm, where each pair of identical feature points on the match is $\left(p_i, p_i'\right)$, and n denotes the total number of identical feature points on the match in ϕ. Therefore, ϕ can be expressed as:

$$\phi = \left\{\left(p_1, p_1'\right), \left(p_2, p_2'\right), \ldots, \left(p_n, p_n'\right)\right\} \tag{20}$$

In this stage of calculation, each geographic alignment calculation unit needs to judge the number of identical feature point pairs n in ϕ to determine whether the number of feature point pairs in ϕ meets the requirements for the next stage of calculation. The threshold value for the number of feature pairs in ϕ that satisfy the conditions for the next stage of calculation is indicated by σ, and the geographic alignment calculation unit that does not satisfy the conditions stops the calculation directly.

(2) Second computation stage

Each geographic alignment calculation unit calculates the corresponding rectangular geographic area of the 3D model on the remote sensing image window slice according to the ϕ obtained in the first calculation stage. In this paper, the random sampling consistency algorithm is used to calculate the pixel coordinates of the top view of the 3D model to the corresponding pixel coordinates conversion matrix on the remote sensing image window slice.

For ϕ obtained in the first stage of computation, let the pixel coordinates of the same feature points on any pair of matches therein be $f_m = (x, y, 1)^T$, $f_s' = \left(x', y', 1\right)^T$, s as scale parameters, respectively, then the pixel

coordinates of the top view of the 3D model to the corresponding pixel coordinate mapping matrix F on the window slice of the remotely sensed image satisfy the following conditions:

$$s \times f_m \sim F \times f_g' = \begin{bmatrix} f_{11} & f_{12} & f_{13} \\ f_{21} & f_{22} & f_{23} \\ f_{31} & f_{32} & f_{33} \end{bmatrix} \times f_g' \tag{21}$$

From ϕ, 4 pairs of identical feature points on the matches are randomly selected and replaced into Eq. (20) to iteratively compute each element in F. For the matrix F obtained from each iteration, the total mapping error is calculated using the following formula. Accordingly, the smaller its value, the more accurate the matrix F obtained from iterative computation. Then:

$$J(\phi) = \sum_{i=1}^{n} \left(x_i - \frac{f_{11}x_i' + f_{12}y_i' + f_{13}}{f_{31}x_i' + f_{32}y_i' + f_{33}} \right)^2 + \left(y_i - \frac{f_{21}x_i' + f_{22}y_i' + f_{23}}{f_{31}x_i' + f_{32}y_i' + f_{33}} \right)^2 \tag{22}$$

After the iterative computation of F, the matrix F corresponding to the minimum value of $J(\phi)$ is the transformation matrix from the pixel coordinates of the top view of the 3D model to the corresponding optimal pixel coordinates on the window slice of the remote sensing image, so that it is M_{MP}. In this paper, the pixel coordinate system of the top view of the 3D model is defined as the model pixel coordinate system, and the pixel coordinate system of the window slice of the remote sensing image is defined as the geographic pixel coordinate system. After that, the pixel coordinates of the four vertices of the top view of the 3D model are transformed to the remote sensing image using M_{MP-GP}. Order:

$$S = \left\{ (0,0,1)^T, (0, w_m, 1)^T, (h_m, 0, 1)^T, (h_m, w_m, 1)^T \right\} \tag{23}$$

is the set of pixel coordinates of the four vertices of the top-left, top-right, bottom-left, and bottom-right corners of the top view of the 3D model, then, its corresponding set of pixel coordinates on the remote sensing image slice S' is:

$$S' = U_{p \in S} M_{MP-GP} \cdot p \tag{24}$$

The four pixel coordinates in S' are connected in sequence, and the shape of the graph generated after the connection is used to determine whether the region is the region of the 3D model on the remote sensing image.

The third computation stage:

The third stage is to geo-align the 3D model by obtaining the geographic coordinates corresponding to all the elements in the 3D model. Without loss of generality, the 3D models from GIS mentioned in this paper are in IFC format and the 3D models from multiple sources in GIS are uniformly converted into 3D grid models in this step. Therefore, in this paper, the 3D mesh model is defined as a collection of triangular faces, and the geometric representation of the 3D mesh model is denoted by M_{tri}, then:

$$M_{tri} = \{ p_1, p_2, \ldots, p_m \}, p_i = (x_i, y_i, z_i) \in R^3 \tag{25}$$

Where $p_i = (x_i, y_i, z_i)$ denotes the vertex coordinates of a triangular face in a triangular mesh model.

Depending on the placement level of all elements in the GIS, the local coordinate system of each element can be converted uniformly to the project-level local coordinate system of the GIS.

3.3 Multi-source geographic information fusion framework

3.3.1 IHS transform image fusion

For the geographic information data in GIS, part of it is the image obtained by using UAV inclined measurement technology, and part of it is the data obtained by remote sensing technology, and there is a certain deviation of the image obtained by different methods, so it needs to be fused to obtain more accurate geographic information. Thus, this paper introduces the HIS transform to fuse the multi-source geographic information data.

The fusion method of IHS transformation mainly transforms the acquired image from the RGB color space to the IHS color space, and processes the luminance component I in the IHS color space, and then inverts the processed component I and the original components H and S together in the IHS inverse transformation to the RGB color space, and ultimately obtains the fusion image that is richer in color and has clearer information about the details of the features.

The conversion relationship between IHS color space and RGB color space is as follows:

(1) RGB space is shifted to IHS space, then:

$$\begin{pmatrix} I \\ v_1 \\ v_2 \end{pmatrix} = \begin{pmatrix} 1/\sqrt{3} & 1/\sqrt{3} & 1/\sqrt{3} \\ 1/\sqrt{6} & 1/\sqrt{6} & -2/\sqrt{6} \\ 1/\sqrt{2} & -1/\sqrt{2} & 0 \end{pmatrix} \begin{pmatrix} R \\ G \\ B \end{pmatrix} \tag{26}$$

In the above equation, v_1 and v_2 represent their components on the Cartesian coordinate system, and the hue H and saturation S can be calculated by the following equation if v_1 and v_2 are known:

$$H = \tan^{-1}\left(\frac{v_2}{v_1}\right) \tag{27}$$

$$S = \sqrt{v_1^2 + v_2^2} \tag{28}$$

(2) IHS space is transferred back to RGB space, then:

$$\begin{pmatrix} R \\ G \\ B \end{pmatrix} = \begin{pmatrix} 1/\sqrt{3} & 1/\sqrt{6} & 1/\sqrt{2} \\ 1/\sqrt{3} & 1/\sqrt{6} & -1/\sqrt{2} \\ 1/\sqrt{3} & -2/\sqrt{6} & 0 \end{pmatrix} \begin{pmatrix} I \\ v_1 \\ v_2 \end{pmatrix} \tag{29}$$

The IHS transform fusion mainly processes the luminance I component after the IHS transform in the following steps:

(1) The low-resolution multispectral image and the high-resolution panchromatic image are respectively transformed by the IHS positive transform, and after the transformation, the three components of each will be obtained, respectively $S_1, H_1, I_1, S_2, H_2, I_2$.

(2) The luminance component of the fused geographic information image is selected to be replaced by the luminance component of the high-resolution panchromatic image, and is expressed as I_1'.

(3) The new luminance component I_1' and the original low-resolution multispectral image S_1, H_1 are inverted by the IHS inverse transform, and finally a clearer geographic information fusion image of the features is obtained.

3.3.2 Data fusion processing flow

Compared with two-dimensional planar data fusion, which mainly considers attribute characteristics, format type and organizational structure, three-dimensional spatial data also need to explore data fusion issues in terms of location information and spatial element relationships. The data gathered in the platform come from a variety of systems and collection routes, covering different industries such as geographic information and water conservancy, resulting in inconsistencies in data structure types, attribute features, projection coordinates, element relationships, etc., and multi-scale variability exists.The multi-source big data fusion process of GIS is shown in Figure 4. In this paper, various types of geographic information data collected are subjected to heterogeneous fusion such as consistency processing, three-dimensional spatialization, and classification into the library, and are respectively injected with spatial, attribute, and temporal three-dimensional identifiers.

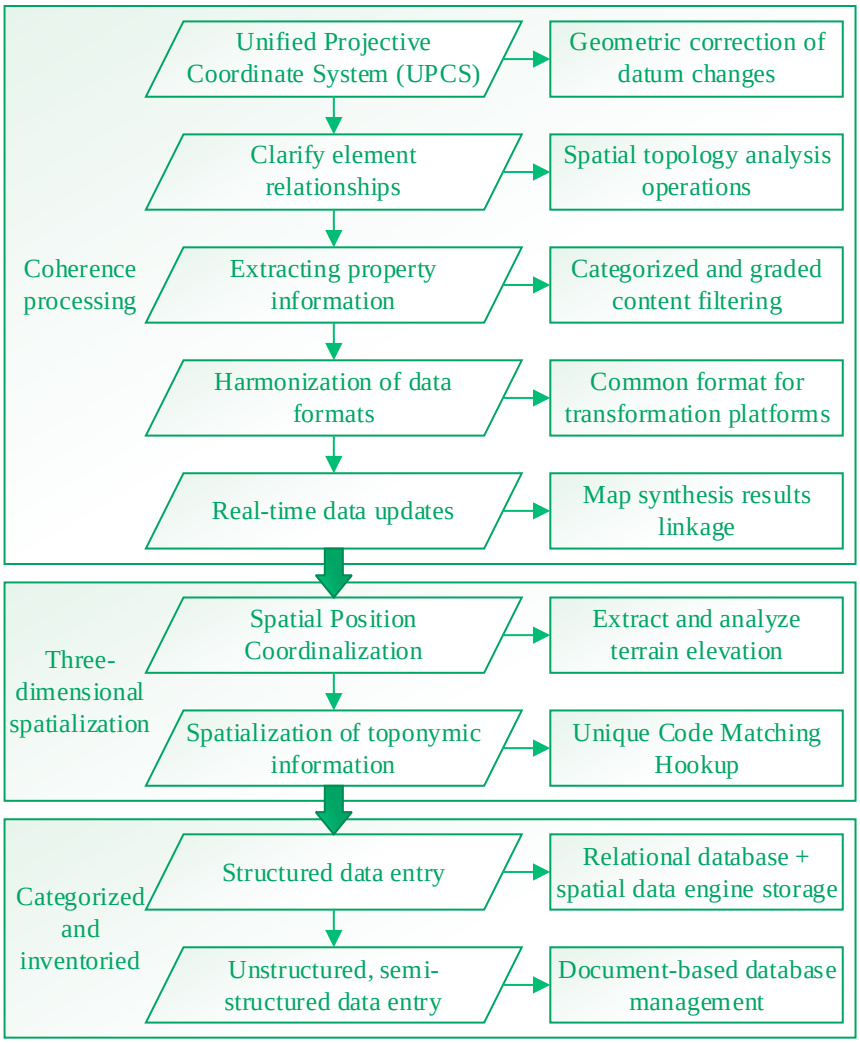

Figure 4 Multi-source data fusion processing process

Encapsulating all kinds of spatial and non-spatial data resources into services and releasing them to the outside world in the form of interfaces can effectively shield the heterogeneity of multi-source data and better adapt to the platform's business needs and the diversification of functional applications. The GIS built after the data fusion

process can unify the management of various types of data calls, solve the problem of heterogeneity of different data, and can be effectively applied to the integration and consolidation of multi-departmental data resources to further enhance the scope of application of GIS.

4. Analysis of the fusion effectiveness of multi-source big data

Geographic data are directly or indirectly related data on a point or area of the earth's surface, natural and social data that represent geographic location and distribution characteristics, and symbolic representations of the relationships between various geographic features and phenomena. The data used in GIS can be broadly categorized into three types, namely, observation data, experimental data and statistical data, according to the way they are obtained. These data are the important foundation and prerequisite for geography research, and at the same time constantly promote the cross-fertilization of geography and its related disciplines. Realizing the effective integration of multi-source data in GIS can enhance the depth analysis of geographic information by GIS and realize the application of GIS in a wider range of fields.

4.1 Validation of geographic information alignment algorithms

4.1.1 Geographic information feature matching

For this paper proposes to utilize SIFT algorithm for feature matching of multi-source data, five groups of multi-rotor UAV images are used to pre-train the algorithm. For each group of UAV impacts, feature points are extracted using the SIFT algorithm, and the 30 most similar images of each image are obtained based on vocabulary tree search to form image matching pairs, which are used to guide the subsequent feature matching. Fig. 5 Geographic information image feature matching results of different algorithms.

The experimental results show that with SIFT as the manual feature matching benchmark, the image block description networks represented by L-Net, GeoDesc and HardNet can all improve the feature matching performance, which is manifested in the improvement of two indexes, namely, the in-point rate and the matching rate.GeoDesc and HardNet both adopt the L-Net network architecture, and based on which they respectively add the difficult negative sample sampling strategy and the GeoDesc and HardNet both adopt the L-Net network architecture and add the difficult negative sample sampling strategy and the loss function design with geometric constraints respectively on this basis, and their performance in terms of inner point rate and matching rate is also improved. The SIFT algorithm proposed in this paper performs better than GeoDesc and HardNet in terms of the interior point rate and matching rate in the remaining four data sets, except that it does not perform as well as GeoDesc in data set 1. For the five sets of experimental data, the maximum improvement of the SIFT algorithm in terms of the interior point rate and the matching rate compared with GeoDesc and HardNet reaches 6.56% and 7.98% respectively. This is due to the fact that the SIFT algorithm wants to extract feature points for geographic information image information and constructs an image pyramid in this way, with the continuous superposition of the number of layers of the pyramid, it will further improve the matching ability of the SIFT algorithm on the feature points of the geographic information image data, so as to realize the detection and description of the joint features of the geographic information image data.

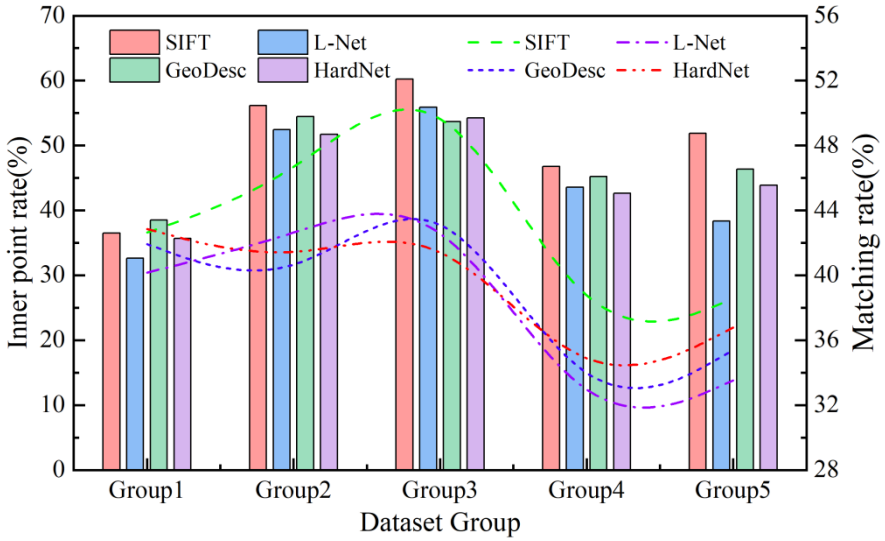

Figure 5 Geographical information image matching results

4.1.2 Stability of the SIFT algorithm

(1) Scale and rotation invariance comparison

In order to test the matching accuracy of this paper's method on geographic information image rotation and scale change, a group of data is randomly selected from five sets of UAV data sets, and the image scale is scaled by 2 times and rotated clockwise by 60°, so that the matching time consumption and accuracy of different algorithms in the case of image rotation and scale change are shown in Table 1.

In the case of geographic information image rotation and scale change, the feature points of geographic information image obtained based on SIFT algorithm have better stability, and still can maintain a high matching accuracy. Its matching time for the feature points of geographic information image is only 1.241s, and its feature point matching accuracy reaches 88.44%, which is 3.77 percentage points higher than that of the best-performing GA-SURF algorithm. This reflects that the geographic information image feature extraction based on the SIFT algorithm in this paper has high stability, and even if the geographic information image has irregularities, the image information can be effectively extracted, which can better cope with the geographic information images acquired by UAVs with different tilt angles.

Table 1 Comparison results after image rotation and scale transformation

Algorithm	Match time	Match point	Correct match	Matching accuracy
SIFT	1.241s	865	765	88.44%
L-Net	2.604s	648	503	77.62%
GeoDesc	2.738s	726	518	71.35%
HardNet	2.752s	739	521	70.50%
ORB	2.158s	614	496	80.78%
SURF	2.437s	663	547	82.50%
GA-SURF	2.915s	672	569	84.67%

(2) Luminance Transformation Comparison

Light intensity change is more common in the actual situation, is one of the important factors affecting image matching. In order to verify the performance of this paper's method of geographic information image matching in

the case of image illumination intensity transformation, further by manually setting the experimental map from dark to bright for comparison experiments, the results are shown in Figure 6.

From the results of geographic information image matching under brightness transformation, it can be seen that with the increase of light intensity all algorithms of geographic information matching accuracy is first increased and then decreased, this paper is based on the SIFT algorithm overall decline is smaller, when the light intensity increases from 1 ° to 5 °, its matching accuracy of geographic information images from 90.01% to 89.24%. Although the other six algorithms have some improvement in matching accuracy when the light intensity is 5° compared with 1°, the improvement is small, and the overall matching accuracy of geographic information images is lower than that of the SIFT algorithm. This also reflects that the method in this paper has good robustness to illumination transformations, and can adapt to the accurate matching of geographic information images acquired under different environments, providing a basis for multi-source heterogeneous data fusion.

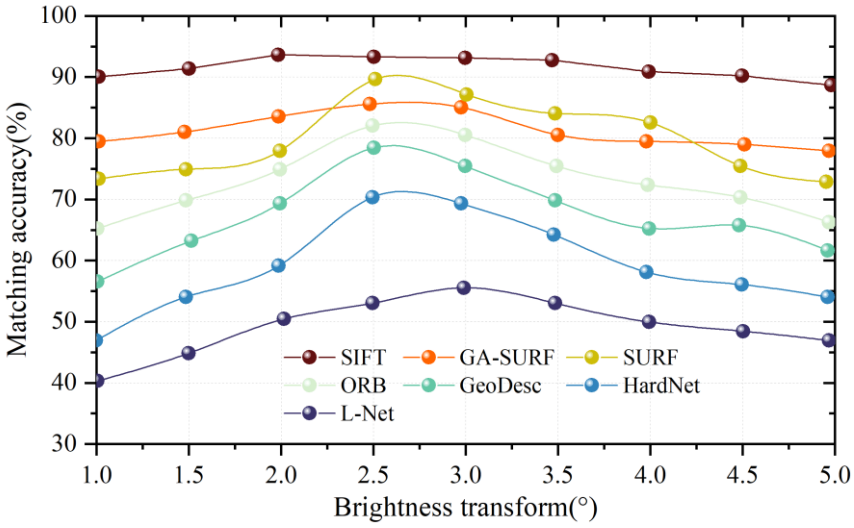

Figure 6 Contrast to brightness

4.2 Multi-source heterogeneous data fusion analysis

4.2.1 Multi-source data fusion experiments

Objective evaluation is the quantitative evaluation and analysis of images using relevant indicators. Since subjective evaluation results can be biased by personal differences, in order to reduce the interference of personal subjectivity and other factors, the use of objective evaluation indicators can evaluate the results scientifically and effectively. For the fusion of remote sensing images and UAV images with geographic information, this paper selects the following four objective evaluation indexes correlation coefficient (CC), average gradient (AG), information entropy (EN) and standard deviation (SD) to evaluate the fused images objectively. Remote sensing images use satellite data, UAV images are image data from section 4.1.1, and IHS transform, WV-SR, NSCT-SM, NSCT-PCNN, and NSST-SR are selected for comparison, resulting in the results of the objective evaluation of geo-information image fusion as shown in Table 2.

In the fusion of multi-source heterogeneous images, CC is to reflect the degree of correlation between the two images, and the closer its value is to 1, the higher the degree of correlation is, AG reflects the characteristics of texture transformation in the fused image, and the larger its value is, the better the image clarity is, EN is used to measure the degree of information richness of the fused image, and SD is the index to reflect the contrast of the fused image, and the larger the values of both SD and EN are, the better the fused image effect is.

As can be seen from the table, the CC of WV-SR fusion algorithm is lower, indicating the presence of large spectral distortion. Compared with the WV-SR fusion algorithm, the IHS fusion algorithm is improved in all the indexes,

and the CC value of 0.924 is the highest among the five fusion algorithms, which indicates that the algorithm does well enough in spectral retention.The NSCT-SM fusion algorithm performs better in spectral retention, but the AG of this algorithm decreases by 0.129 compared with the WV-SR fusion algorithm, and the clarity of fused image still needs to be enhanced. Clarity still needs to be enhanced.The NSCT-PCNN fusion algorithm has improved all the indexes compared to WV-SR and NSCT-SM algorithms, which indicates that the spectral and spatial information in the fused image is better maintained. The algorithm in this paper has obvious advantages in fused image effect compared with the other four algorithms, in which the EN value of the algorithm is improved by 7.13%, 4.00%, 3.32%, and 5.33% compared with the other four algorithms, respectively. It shows that the geographic information image obtained by IHS transform contains the most information, and the spatial detail information is maintained better, and the improvement of CC value also indicates that the spectral distortion of geographic information image is minimized, and the fusion image quality is optimal. Taken together, the IHS transform fusion algorithm has the best fusion effect, better realizes the fusion image in the spectral retention and spatial detail retention of the equilibrium, and is an effective algorithm for the fusion of geo-information remote sensing images and UAV images with multi-source heterogeneous data.

Table 2 Objective evaluation of geographic information image fusion

Algorithm	CC	AG	EN	SD
IHS	0.924	7.516	7.652	45.268
WV-SR	0.813	6.157	7.143	36.732
NSCT-SM	0.847	6.028	7.358	38.415
NSCT-PCNN	0.885	7.214	7.406	41.206
NSST-SR	0.862	6.359	7.265	37.494

4.2.2 Three-dimensional reconstruction of geographic information

After fusion of remote sensing and UAV image data using the HIS transform fusion algorithm, the fused data are displayed in GIS in three dimensions. First, the real monitoring point of the scene in reality is established and the detailed orientation of the real checkpoint is found in the real model. Then use Acute3D Viewer software to make two sides of the coordinates of this check point and take it as the model coordinates and record it as X', Y', Z'.

Take the acquired coordinates of the measured check point as the real coordinates and record it as X, Y, Z. Then the accuracy of the geographic information 3D scene is shown in Table 3.

According to the relevant specifications of the 3D geographic information model, the planar accuracy for the mapping scale of 1:1000 is required to be within 0.5m, and the elevation accuracy error is within 0.8m. From the data in the table, the maximum error of the 3D model of geographic information obtained through the fusion of heterogeneous data from multiple sources is 0.07m, and the minimum error is 0.01m, which is significantly obtained by the relevant specifications of the 3D geographic information model. This reflects the effectiveness of the multi-source heterogeneous geographic information data fusion method proposed in this paper in GIS, which is able to display the geographic information in front of the user by means of a three-dimensional model, help the user better understand the geographic information situation, and improve the accuracy and practicality of GIS.

Table 3 Precision statistics of 3D geographic information model (m)

Point	X	Y	Z	X'	Y'	Z'	Error
P1	254306.37	352297.12	54.41	254306.32	352297.14	54.43	[-0.02,0.05]
P2	254301.26	352296.57	29.48	254301.28	352296.59	29.46	[-0.02,0.02]
P3	254307.52	352296.24	50.36	254307.54	352296.26	50.33	[-0.02,0.03]

P4	254302.01	352296.45	43.52	254302.06	352296.42	43.55	[-0.05,0.03]
P5	254305.78	352297.36	35.21	254305.73	352297.38	35.26	[-0.05,0.05]
P6	254306.93	352295.93	38.04	254306.89	352295.95	38.05	[-0.02,0.04]
P7	254301.38	352295.68	54.19	254301.36	352295.67	54.12	[0.01,0.07]
P8	254306.54	352294.66	40.34	254306.57	352294.61	40.36	[-0.03,0.05]
P9	254307.61	352297.43	52.68	254307.63	352297.45	52.65	[-0.02,0.03]
P10	254302.25	352296.69	34.93	254302.28	352296.62	34.94	[-0.03,0.07]
P11	254302.38	352295.84	43.56	254302.35	352295.85	43.58	[-0.02,0.03]
P12	254301.53	352296.18	54.87	254301.56	352296.21	54.84	[-0.03,0.03]

5. Conclusion

This paper establishes a geographic information system in C/S and B/S modes, and analyzes the mechanism of multi-source data fusion in GIS, and fuses remote sensing images and unmanned aerial vehicle (UAV) images with geographic information three-dimensional modeling technology combined with distributed geographic information alignment algorithms and HIS transformed images, to provide support for the display of three-dimensional geographic information in GIS.

(1) This paper utilizes the SIFT algorithm for geographic information image alignment, and the algorithm in this paper achieves the maximum improvement of 6.56% and 7.98% in the internal point rate and matching rate compared with GeoDesc and HardNet, respectively. The matching time of geographic information image feature alignment using SIFT algorithm is only 1.241s, and its feature point matching accuracy reaches 88.44%. The SIFT algorithm can effectively obtain the geographic information image features under different scales and light intensity conditions, which fully satisfies the accurate processing of geographic information images under different conditions.

(2) When image fusion is performed based on HIS transform, its CC value is 0.924, and the EN value is 3.32% higher than that of the best-performing NSCT-PCNN. This reflects that the HIS transform can fully retain the image features when fusing remote sensing images and UAV images, and the spectral loss of the fused geographic information image is minimized.

(3) Based on the specification of 3D scene modeling, the maximum error of the geographic information 3D model after fusion of multi-source heterogeneous data in this paper is only 0.07 m, and the minimum error is 0.01 m. It shows that a more accurate 3D model of geographic information can be obtained by using the multi-source geographic information data fusion framework proposed in this paper, which supports the realization of a wide range of GIS applications.

References

[1] Trivedi, A. , Rao, K. V. R. , Rajwade, Y. , Yadav, D. , & Verma, N. S. . (2022). Remote sensing and geographic information system applications for precision farming and natural resource management. Indian Journal of Ecology.

[2] Hai, D. T. , & Phin, T. T. . (2022). Utilization of geographic information system (gis) for urban management of rachgia city, vietnam. Archives of civil engineering.

[3] Lu, C. , & Wen, F. . (2018). Geographic information system query optimisation algorithm based on redundant data deletion and filtering technology. International journal of internet protocol technology, 11(4), 250-256.

[4] Zhu, W. , Hou, Y. , Wang, E. , & Wang, Y. . (2020). Design of geographic information visualization system for marine tourism based on data mining. Journal of Coastal Research, 103(sp1), 1034.

[5] Wang, W. , Wu, X. , He, A. , & Chen, Z. . (2019). Modelling and visualizing holographic 3d geographical scenes with timely data based on the hololens. International Journal of Geo-Information, 8(12), 539.

[6] Leon-Garza, H. , Hagras, H. , Pena-Rios, A. , Conway, A. , & Owusu, G. . (2022). A type-2 fuzzy system-based approach for image data fusion to create building information models. Information Fusion.

[7] Rahimi, Sohrab, Martin, Michael, J. R. , Obeysekere, & Eric, et al. (2017). A geographic information system (gis)-based analysis of social capital data: landscape factors that correlate with trust. Sustainability.

[8] Pan, Shaoming, Zhengquan, Meng, Qingxiang, & Chong, et al. (2017). A combination replication strategy for data-intensive services in distributed geographic information system. International Journal of Distributed Sensor Networks, 13(5), 1-1.

[9] Rabie, A. , Peterson, E. , Kostelnick, J. , & Rowley, R. . (2017). Optimizing digital elevation model resolution inputs and number of stream gauges in geographic information system predictions of flood inundation: a case study along the illinois river, usa. Environmental and Engineering Geoscience(4).

[10] Peng, C. , Cai, Y. , Liu, G. , & Liao, T. W. . (2020). Developing a reliability model of cnc system under limited sample data based on multisource information fusion. Mathematical Problems in Engineering.

[11] Brumancia, E. , Justin Samuel, S. , Gladence, L. M. , & Rathan, K. . (2019). Hybrid data fusion model for restricted information using dempster–shafer and adaptive neuro-fuzzy inference (dsanfi) system. Soft Computing.

[12] Chen, Y. , Wang, C. , Zhou, Y. , Zuo, Y. , Yang, Z. , & Li, H. , et al. (2024). Research on multi-source heterogeneous big data fusion method based on feature level. International Journal of Pattern Recognition and Artificial Intelligence, 38(02).

[13] Nguyen, M. H. , Armoogum, J. , & Adell, E. . (2021). Feature selection for enhancing purpose imputation using global positioning system data without geographic information system data:. Transportation Research Record, 2675(5), 75-87.

FUNDING

China Geological Survey“Big data intelligent prospecting prediction（Yantai Center）”project(DD20242837)

ABOUT THE AUTHOR

Jing Zhang:a.Yantai Center of Coastal Zone Geological Survey, China Geological Survey, Yantai 264000, Shandong, China

b. Ministry of Natural Resources Observation and Research Station of Land-Sea Interaction Field in the Yellow River Estuary,Yantai 264000, Shandong,China

E-mail: zhangjzhang2024@163.com

Yonghui Yin:a.Yantai Center of Coastal Zone Geological Survey, China Geological Survey, Yantai 264000, Shandong, China

b. Ministry of Natural Resources Observation and Research Station of Land-Sea Interaction Field in the Yellow River Estuary,Yantai 264000, Shandong,China

E-mail: y2h521@163.com

Pengfei Zhao:a.Yantai Center of Coastal Zone Geological Survey, China Geological Survey, Yantai 264000, Shandong, China

b. Ministry of Natural Resources Observation and Research Station of Land-Sea Interaction Field in the Yellow River Estuary,Yantai 264000, Shandong,China

E-mail:bingguojingjing@163.com